Neurobiology of Aging 132 (2023) 198–208

Contents lists available at ScienceDirect

Neurobiology of Aging

journal homepage: www.elsevier.com/locate/neuaging.org

Regular article

Degeneration of cholinergic white matter pathways and nucleus basalis of Meynert in individuals with objective subtle cognitive impairment

Tiantian Qiu [a,1], Hui Hong [b,1], Qingze Zeng [b], Xiao Luo [b], Xiaohan Wang [c], Xiaopei Xu [b], Fei Xie [d], Xiaodong Li [a], Kaicheng Li [b], Peiyu Huang [b], Shouping Dai [a,*,2], Minming Zhang [b,**,2], for the Alzheimer's Disease Neuroimaging Initiative

[a] Department of Radiology, Linyi People's Hospital, Linyi, China
[b] Department of Radiology, The Second Affiliated Hospital of Zhejiang University School of Medicine, Hangzhou, China
[c] Clinical Laboratory, Linyi Central Hospital, Linyi, China
[d] Department of Equipment and Medical Engineering, Linyi People's Hospital, Linyi, China

ARTICLE INFO

Article history:
Received 19 June 2023
Revised 19 September 2023
Accepted 20 September 2023
Available online 25 September 2023

Keywords:
Alzheimer's disease
Objective subtle cognitive impairment
Cholinergic system
Nucleus basalis of Meynert
Magnetic resonance imaging

ABSTRACT

We evaluated alterations in the nucleus basalis of Meynert (NBM) volume and integrity of cholinergic white matter pathways in objective subtle cognitive impairment (Obj-SCI) individuals. NBM segmentation and cholinergic pathways tracking were conducted at baseline, 12-, 24-, and 48-month follow-ups in 41 Obj-SCI individuals and 61 healthy controls (HC). The baseline and 4-year rate of change in NBM volume and cholinergic pathways mean diffusivity were compared. Associations between cholinergic index changes and pathological processes and cognitive performance were evaluated. After controlling for age, sex, *APOE* genotype, and total intracranial volume, Obj-SCI individuals exhibited reduced NBM volume and increased medial pathway mean diffusivity compared to HC at baseline. Furthermore, amyloid-positive Obj-SCI individuals exhibited a steeper longitudinal decline in NBM volume than HC. Additionally, decreases in NBM volume and cholinergic pathways integrity were associated with amyloid and vascular pathologies and cognitive decline. Overall, degeneration of the cholinergic system plays an important role in cognitive impairment during the preclinical stage of Alzheimer's disease, which may provide a significant target for early therapeutic interventions.

1. Introduction

Early detection of cognitive impairment in the preclinical stage has been a major concern of Alzheimer's disease (AD) research, as it provides the best opportunity to implement interventions and treatments to halt the disease progression (Dubois et al., 2016). In this context, Thomas et al. (2018) proposed new actuarial criteria that can capture objective subtle cognitive decline in the preclinical stage of AD using sensitive neuropsychological measures. It is defined by performance >1 standard deviation below the

Abbreviations: Aβ, amyloid beta; AD, Alzheimer's disease; ADNI, Alzheimer's disease neuroimaging initiative; ANTs, advanced normalization tools; AVLT, auditory verbal learning test; BF, basal forebrain; BNT, Boston naming test; CAT, computational anatomy toolbox; CSF, cerebrospinal fluid; DTI, diffusion tensor imaging; FDR, false discovery rate; FLAIR, fluid-attenuated inversion recovery; FLIRT, FMRIB's Linear Image Registration Tool; FODs, fiber-orientation distributions; GM, gray matter; IR-SPGR, inversion-recovery spoiled gradient recalled; MCI, mild cognitive impairment; MD, mean diffusivity; MNI, Montreal Neurological Institute; MRI, magnetic resonance imaging; NBM, nucleus basalis of Meynert; Obj-SCI, objective subtle cognitive impairment; PET, positron emission tomography; ROIs, regions of interest; SCD, subjective cognitive decline; SE-EPI, spin echo pulse sequence echo-planar-imaging; SPM, statistical parametric mapping; SS3T-CSD, 3-tissue constrained spherical deconvolution; SUVR, standardized uptake value ratio; SVF, semantic verbal fluency; TE, echo time; TIV, total intracranial volume; TMT, trail-making test; TR, repetition time; WM, white matter; WMH, white matter hyperintensities

* Corresponding author at: Department of Radiology, Linyi People's Hospital, No. 27 East Section of Jiefang Road, Lanshan District, Linyi 276000, China, 5398225769.
** Corresponding author at: Department of Radiology, The Second Affiliated Hospital of Zhejiang University School of Medicine, No. 88 Jiefang Road, Shang-cheng District, Hangzhou 310009, China, 57187315255.
E-mail addresses: daishouping@sina.cn (S. Dai), zhangminming@zju.edu.cn (M. Zhang).
[1] These authors have contributed equally to this work and share first authorship.
[2] These authors have contributed equally to this work and share senior authorship.

https://doi.org/10.1016/j.neurobiolaging.2023.09.011

demographically adjusted (age, sex, and education) mean on (1) 2 neuropsychological measures in 2 different cognitive domains; (2) 2 process scores; or (3) 1 neuropsychological measure and 1 process score. In a 10-year follow-up study, individuals with objective subtle cognitive decline developed mild cognitive impairment (MCI) at a rate 2.5–3.4 times faster than normal controls (Thomas et al., 2018). Although objective subtle cognitive decline has been shown to be associated with rapid amyloid accumulation and neurodegeneration (Thomas et al., 2020), the rigorous neural mechanisms behind it still need to be further explored.

Research spanning several decades strongly suggests that degeneration of the cholinergic system is one of the initial pathophysiological events in AD, and it is linked to cognitive decline (Hampel et al., 2018). Early postmortem studies (Whitehouse et al., 1981, 1982) showed a significant loss of cholinergic neurons in the basal forebrain (BF), particularly the nucleus basalis of Meynert (NBM), in AD patients. The NBM provides the major projections to neocortical areas, amygdala, and hippocampus (Liu et al., 2015). Using specific cholinergic markers, 2 organized white matter (WM) fiber bundles from the NBM to the cerebral cortex were identified as the medial and lateral cholinergic pathways (Selden et al., 1998). Neuroimaging-derived measures of NBM volume and cholinergic pathways microstructures offer the potential to evaluate degeneration of the cholinergic system in the human brain. Patients with MCI and AD had reduced NBM volume compared to healthy controls (HC) (Cantero et al., 2017; Grothe et al., 2012; Herdick et al., 2020), which was a significant predictor of cognitive decline (Teipel et al., 2018) and dementia conversion (Brueggen et al., 2015). Recently, several studies (Nemy et al., 2023; Schumacher et al., 2022, 2023) have successfully tracked the cholinergic pathways in vivo and further found that the integrity of cholinergic pathways is disrupted not only in MCI and AD patients but also in individuals with subjective cognitive decline (SCD). What remains unknown, however, is whether and how the integrity of the cholinergic system is altered in individuals with subtle cognitive decline.

Therefore, we aimed to investigate cholinergic alterations in NBM volume and WM pathways microstructures in individuals with subtle cognitive decline, both cross-sectionally and longitudinally. Additionally, amyloid aggregation and vascular injury are main pathological processes affecting the integrity of the cholinergic system in aging (Cedres et al., 2022). Thus, we further explored the associations between cholinergic indices changes and these 2 pathologies. Finally, the relationships between cholinergic indices and cognitive performance were also investigated.

2. Methods

2.1. Study participants

The data utilized for this study were gathered from the Alzheimer's disease neuroimaging initiative (ADNI) database (http://adni.loni.usc.edu/), an ongoing project that commenced in 2003 with the aim of identifying clinical, neuropsychological, and neuroimaging biomarkers for early disease detection and progression monitoring of AD. Briefly, participants in the ADNI database were between 55 and 90 years old, had ≥6 years of education, a Geriatric Depression Scale score < 6, a modified Hachinski ischemic score ≤4, and had no significant systemic or neurological disease.

2.2. Cognitive groups

To avoid any confusion with the well-established acronym "SCD" for subjective cognitive decline, we used the term "Obj-SCI" for objective subtle cognitive impairment in our study. According to our previously published article (Qiu et al., 2022), 1380 nondemented participants who completed baseline neuropsychological assessments were initially included. Of these participants, 653 who met MCI criteria according to Jak/Bondi actuarial neuropsychological criteria (Bondi et al., 2014; Jak et al., 2009) were excluded. The remaining participants were determined as Obj-SCI or HC status. Participants were classified as Obj-SCI if they performed > 1 SD below the age/sex/education-adjusted mean on: (1) 1 impaired neuropsychological measure score in 2 different cognitive domains (memory, attention/executive function, and language); (2) 2 impaired process scores in auditory verbal learning test (AVLT); or (3) 1 impaired neuropsychological measure score and 1 impaired process score (Thomas et al., 2018). Six neuropsychological measures were used for Obj-SCI classification, consisting of 2 *memory* measures (AVLT delayed free recall correct responses and AVLT recognition [hits minus false-positives]), 2 *attention/executive function* measures (trail-making test [TMT] parts A and B times to completion), and 2 *language* measures (semantic verbal fluency [SVF] total score and 3 0-item Boston naming test total correct). Three process scores were obtained from the AVLT, including *learning slope* ([list A trial 5–list A trial 1]/5), *retroactive interference* (list A trial 6/list A trial 5), and *total intrusion errors* (total number of extra-list intrusion errors across all recall trials). Participants who did not meet the MCI and Obj-SCI criteria were considered to be HC: (1) no impaired neuropsychological measure and process score, (2) 1 impaired neuropsychological measure score, or (3) 1 impaired process score.

To analyze changes in the cholinergic system, we finally included 43 Obj-SCI and 62 HC participants who had available baseline T1-weighted imaging and diffusion tensor imaging (DTI).

2.3. APOE genotyping

APOE genotype was determined by genotyping the 2 single-nucleotide polymorphisms (rs429358, rs7412) that define the *APOE*-ε2, ε3, and ε4 alleles. DNA was extracted by genics from a 3-mL aliquot of EDTA blood (adni.loni.usc.edu/data-samples/genetic-data/). Participants who had 1 or more ε4 alleles were identified as *APOE* ε4 carriers. The genotypes of the Obj-SCI and HC groups were presented in Supplementary Table 1.

2.4. Amyloid PET acquisition and analyses

The amyloid positron emission tomography (PET) images underwent a standardized preprocessing procedure by the ADNI-PET core. The standardized uptake value ratio was determined by averaging the uptake values of the frontal, angular/posterior cingulate, lateral parietal, and temporal cortices, which were then divided by the mean uptake values of the cerebellum. The amyloid beta (Aβ) positivity (Aβ+) was defined as indicated in prior research (Landau et al., 2012), with standardized uptake value ratio ≥1.11 considered positive. The Obj-SCI and HC participants were then separated into 2 subgroups, namely Aβ+ and Aβ negativity (Aβ−). Finally, the study included HC−, Obj-SCI−, and Obj-SCI+ subgroups for the amyloid-stratified analysis.

2.5. MRI acquisition

All participants underwent whole-brain magnetic resonance imaging (MRI) scans using 3 T MRI scanners (GE Medical Systems) according to the ADNI protocol. The T1-weighted and DTI data were acquired at baseline, 12-, 24-, and 48-month follow-up visits. The sequence parameters of T1-weighted inversion-recovery spoiled gradient recalled images were: repetition time (TR) = 6.96 ms, echo time (TE) = 2.8 ms, voxel size = 1.01 × 1.01 × 1.2 mm^3, matrix size = 256 × 256, and flip angle = 11°. The DTI images were acquired using spin echo pulse sequence echo-planar-imaging with the

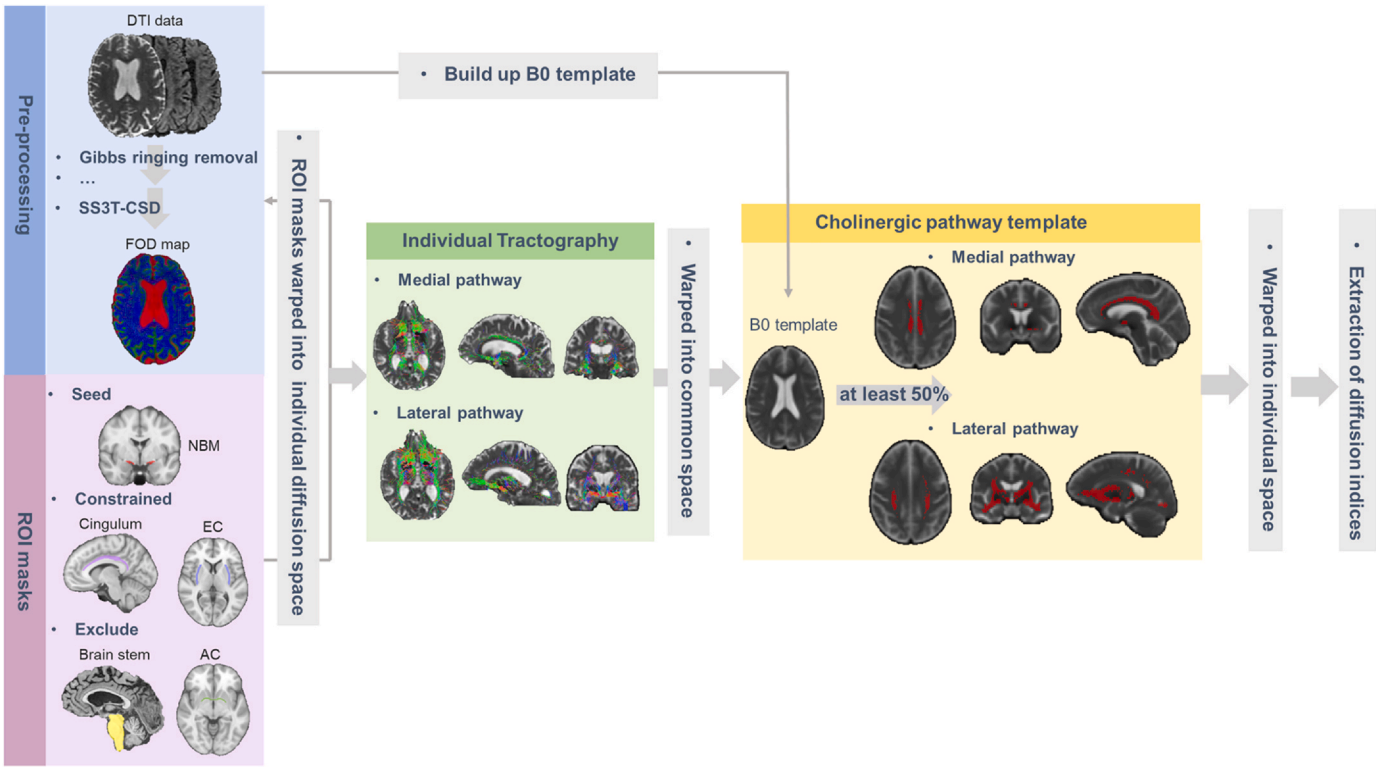

Fig. 1. Flow diagram of cholinergic WM pathways analysis. Abbreviations: AC, anterior commissure; EC, external capsule; FOD, fiber-orientation distributions; NBM, nucleus basalis of Meynert; ROI, regions of interest; SS3T-CSD, single-shell, 3-tissue constrained spherical deconvolution.

following parameters: TR = 9000 ms, voxel size = 2.7 × 2.7 × 2.7 mm^3, matrix size = 256 × 256, flip angle = 90°, and the number of slices = 59. There are 46 separate images for each DTI scan: 5 T2-weighted images with no diffusion sensitization (b0 images) and 41 diffusion-weighted images (b = 1000 s/mm^2). The T2 fluid-attenuated inversion recovery was obtained only at baseline using an echo-planar imaging sequence with the following parameters: TR = 9000 ms, TE = 90 ms, TI = 2500 ms, number of slices = 42, and slice thickness = 5 mm. After screening, 2 Obj-SCI participants and 1 HC participant were excluded due to poor image quality of the DTI data.

2.6. Cholinergic WM pathways analysis

The methods for tracking the cholinergic WM pathways are described below (Fig. 1), largely following the procedure described in a previous study (Nemy et al., 2020).

2.6.1. Preprocessing

The DTI data were preprocessed using MRtrix3 (http://www.mrtrix.org) to remove Gibbs ringing and correct for eddy current, head motion, and bias field. Subsequently, fiber-orientation distributions were determined for each participant using single-shell, 3-tissue constrained spherical deconvolution (Dhollander and Connelly, 2016). The 3-tissue response functions were estimated directly from the diffusion MRI data themselves and then averaged to obtain a group average anisotropic single-fiber WM response function and isotropic gray matter (GM) and cerebrospinal fluid (CSF) response functions using an unsupervised method (Dhollander et al., 2016). Finally, bias field correction and intensity normalization in the log-domain were performed on the 3-tissue compartments.

2.6.2. Regions of interest masks

Following the methodology described previously (Nemy et al., 2020), 5 regions of interest (ROIs) masks for cholinergic tractography were selected. The NBM ROI was obtained from the Montreal Neurological Institute space, which includes the anterior lateral, intermediate, and posterior regions of the NBM region of the BF mask (Kilimann et al., 2014; Schumacher et al., 2022). The cingulum and external capsule ROIs were selected from the Johns Hopkins University WM atlas. An experienced neuroradiologist (Q.T.) delineated the anterior commissure ROI mask in the Montreal Neurological Institute template. To obtain the brainstem masks, advanced normalization tools (ANTs, http://stnava.github.io/ANTs/) segmentation tool was used. Briefly, the "antsBrainExtraction.sh" script was firstly employed for skull stripping, effectively removing nonbrain tissues. Subsequently, the "antsRegistrationSyN.sh" script was applied to register individual skull-stripped T1 images with the Oasis template (https://github.com/brainspaces/OASIS). Finally, the "antsAtroposN4.sh" script was used for tissue segmentation. This step divided the brain into 6 distinct tissue categories: GM, WM, CSF, deep GM, cerebellum, and brainstem regions.

To perform tractography, all masks should be registered into individual diffusion space. For this regard, the NBM, cingulum, external capsule, and anterior commissure ROI masks were first registered into individual T1 space using a nonlinear SyN registration algorithm (Avants et al., 2008) in ANTs. Subsequently, these required individual T1 space ROI masks were further registered into individual diffusion space using FMRIB's linear image registration tool (Ashburner and Friston, 2007).

2.6.3. Individual tractography

Individual tractography was performed on all HC participants using tckgen in MRtrix. Specifically, the NBM ROI mask was designated as the seed mask, while the brainstem and anterior

commissure ROI masks were excluded. To track the cholinergic medial and lateral pathways, the cingulum and external capsule ROI masks were used as inclusion masks, respectively. The parameters for tractography are: tractography algorithm: iFOD2; number of generated streamlines: 10,000; all other parameters, such as step size and angle constraints, were set to default values by MRtrix.

2.6.4. Cholinergic pathway templates

The B0 template was first generated using the preprocessed B0 images of all cognitively normal participants through the "build-template" module in ANTs. The medial and lateral pathways in the individual space were then transformed into this common space. Subsequently, only the voxels that appeared in a minimum of 50% of the cases were preserved. This resulted in the final cholinergic pathway templates (Schumacher et al., 2022).

2.6.5. Individual cholinergic pathway

Using the cholinergic pathway templates, the individual medial and lateral pathways were warped into their respective individual spaces. Finally, the proper positioning of all individual pathways was verified through manual inspection.

2.6.6. Extraction of diffusion indices

The average mean diffusivity (MD) index, which has previously been demonstrated to be sensitive to injury of cholinergic pathways (Nemy et al., 2020, 2023; Schumacher et al., 2022), was utilized to characterize the microstructural properties of the cholinergic WM pathways. Specifically, the mean MD value across all voxels within the cholinergic WM pathways was calculated to assess their integrity.

2.7. NBM volumes

The T1-weighted images were preprocessed and analyzed using the computational anatomy toolbox (CAT12, http://dbm.neuro.unijena.de/cat/) and statistical parametric mapping 12 (SPM12, http://www.fil.ion.ucl.ac.uk/spm/software/spm12/). The images were bias-corrected, tissue-classified (GM, WM, and CSF), and registered using linear (12-parameter affine) and nonlinear transformations (warping) using the CAT12 default preprocessing pipeline. Mean GM volumes were calculated within the NBM mask. Additionally, NBM volume was normalized by the total intracranial volume (TIV) to adjust for interparticipant variability in brain size. The estimation of TIV was performed using CAT12. The T1 structural images were subjected to preprocessing steps for the correction of magnetic inhomogeneity, skull strip, and tissue segmentations. The TIV was calculated as the sum of WM, GM, and CSF.

2.8. WMH volumes

WM hyperintensities (WMH) were segmented based on the T2 fluid-attenuated inversion-recovery images. The lesion segmentation tool was used to automatically segment the WMH using a lesion prediction algorithm based on SPM12 (https://www.applied-statistics.de/lst.html) (Schmidt et al., 2012). The WMH images created automatically were manually corrected to avoid any inaccuracies in segmentation. The lesion segmentation tool then automatically extracted the WMH volumes. Eventually, the WMH volumes were normalized to TIV and transformed using a natural logarithm to meet the assumption of normal distribution for analysis.

2.9. Statistical analysis

Statistical analyses for demographic and clinical data were conducted using SPSS statistical software (version 26; SPSS, Inc, Chicago, IL). A 2-tailed $p < 0.05$ was considered statistically significant. Age, years of education, neuropsychological measures, and WMH volume were compared between the HC and Obj-SCI groups using independent *t*-tests. The χ^2 test was used for categorical variables, including sex, *APOE* genotype, and Aβ positivity. Moreover, the demographics and clinical variables mentioned above were also compared in the amyloid-stratified subgroups by employing a 1-way analysis of variance, followed by the Bonferroni multiple comparison correction.

After adjusting for age, sex, *APOE* genotype, and TIV, the integrity of the cholinergic system, including both NBM volume and WM pathways MD, was compared between HC and Obj-SCI groups via independent *t*-tests. In the amyloid-stratified subgroups, independent *t*-tests with a false discovery rate multiple comparisons correction ($p < 0.05$) were used to compare the cholinergic system integrity between the HC−, Obj-SCI−, and Obj-SCI+ subgroups.

Linear mixed models were used to examine longitudinal changes in the cholinergic system using the "lme4" package in R 3.0.3 with Rstudio (Bates et al., 2015). Initially, the longitudinal changes in the cholinergic system between the HC and Obj-SCI groups were assessed. The model encompassed several fixed effects, such as age, sex, *APOE* genotype, group (HC vs. Obj-SCI), time (measured in years from baseline), and group × time, while time was modeled as a random effect (random intercepts and slopes) for each participant. Three indices were examined dependently, namely normalized NBM volume (TIV-corrected), medial pathway MD, and lateral pathway MD. Subsequently, the same analysis was further tested in the amyloid-stratified subgroups.

A step-wise linear regression model was employed to examine the impact of pathological processes, specifically amyloid aggregation and WMH burden, on cholinergic indices across all participants, using age, sex, education, and *APOE* genotype as covariates. Standardized regression coefficients were conducted to assess the influence of each pathology.

Finally, a partial correlation analysis was conducted to examine the relationship between cholinergic indices and cognitive performance across all participants with age, sex, education, and *APOE* genotype as covariates.

3. Results

3.1. Demographic and clinical data

Demographic characteristics, cognitive performance, and WMH volume for 61 HC and 41 Obj-SCI participants are shown in Table 1. There were no significant differences in age, sex, and education level between the HC and Obj-SCI groups. However, the Obj-SCI group had a higher frequency of *APOE* ε4 carriers ($p = 0.009$) compared to the HC group. Meanwhile, the Obj-SCI group exhibited significantly lower scores than the HC group in almost all neuropsychological measures, consistent with expectations. There was no significant difference in WMH volume between the 2 groups. The demographic and clinical data for the amyloid-stratified subgroups were presented in Supplementary Table 2.

3.2. Group comparison of cholinergic NBM and WM pathways at baseline

A comparison between groups of cholinergic NBM and WM pathways at baseline is shown in Fig. 2. The analysis revealed that the Obj-SCI group had a decrease in NBM volume ($p = 0.035$, Fig. 2A) and an increase in MD of the medial pathway ($p = 0.004$, Fig. 2B) compared to the HC group after controlling for age, sex, *APOE* genotype, and TIV. However, no significant difference was detected in MD of the lateral pathway between groups ($p = 0.089$, Fig. 2C).

Table 1
Baseline demographic and clinical information

	HC (N = 61)	Obj-SCI (N = 41)	T-value/χ2-value	*p*-value
Age, years	72.81 (6.63)	73.58 (6.36)	−0.58	0.561
Sex (F/M)	33/28	18/23	1.02	0.313
Education, years	16.66 (2.74)	16.02 (2.64)	1.16	0.250
APOE ε4 carriers, n (%)	17 (27.9%)	22 (53.7%)	6.91	0.009
Cerebral Aβ levels[a]	1.12 (0.18)	1.17 (0.23)	−1.37	0.176
Aβ positivity, n (%)	19 (31.7%)	19 (46.3%)	2.24	0.135
MMSE	29.03 (1.32)	28.27 (1.75)	2.38	0.020
Memory				
AVLT delayed recall	8.59 (3.51)	4.54 (2.98)	6.07	< 0.001
AVLT recognition	27.69 (2.06)	26.44 (2.17)	2.94	0.004
Attention/executive function				
TMT-A (s)	32.11 (10.56)	35.32 (9.25)	−1.58	0.118
TMT-B (s)	76.89 (23.25)	90.24 (34.68)	−2.16	0.034
Language				
SVF	22.11 (4.80)	18.71 (4.91)	3.48	< 0.001
BNT	28.39 (1.67)	28.00 (1.94)	1.1	0.276
AVLT process scores				
Learning slope	1.24 (0.43)	0.92 (0.45)	3.58	< 0.001
Retroactive interference	0.84 (0.20)	0.61 (0.25)	4.96	< 0.001
Total intrusion errors	1.79 (1.83)	2.93 (2.35)	−2.62	0.011
TIV, cm^3	1465.52 (134.52)	1448.89 (139.27)	0.6	0.548
Log-transformed WMH volume (TIV-corrected)	−2.53 (0.40)	−2.53 (0.49)	0.01	0.991

Note: Values are expressed as mean (standard deviation), number of participants.
Key: Aβ, amyloid beta; AVLT, auditory verbal learning test; BNT, Boston naming test; HC, healthy controls; MMSE, mini-mental state examination; Obj-SCI, objective subtle cognitive impairment; SVF, semantic verbal fluency; TIV, total intracranial volume; TMT, trail-making test; WMH, white matter hyperintensities.
[a] 60 HC and 41 Obj-SCI participants had Aβ data.

The amyloid-stratified analysis showed comparable outcomes, whereby a reduction in NBM volume ($p = 0.040$, Fig. 2D) and an elevation in MD of the medial pathway ($p = 0.025$, Fig. 2E) were shown in the Obj-SCI+ group compared to the HC− group. Notably, the Obj-SCI− group also demonstrated a trend of statistically significant increase in MD of the medial pathway relative to the HC− group ($p = 0.054$, Fig. 2E). However, there was no significant difference in MD of the lateral pathway between the groups; see details in Fig. 2F.

3.3. Longitudinal trajectories of cholinergic NBM and WM pathways changes

The longitudinal evolution of cholinergic NBM and WM pathways is shown in Fig. 3. The Obj-SCI and HC groups showed a significant decrease in normalized NBM volume ($p < 0.001$, Fig. 3A) and an increase in both medial and lateral pathway MD (medial pathway: $p < 0.001$, Fig. 3B; lateral pathway: $p = 0.001$, Fig. 3C) over time. However, there were no differences of longitudinal rates between groups ($p = 0.484$, 0.780, and 0.257, respectively).

The amyloid-stratified analysis showed that the Obj-SCI+ group exhibited a more rapid decline in normalized NBM volume than the HC− group ($p = 0.045$), while there was no difference between the Obj-SCI− group and HC− group ($p = 0.530$). Regarding cholinergic WM pathways degeneration, we observed no significant difference in the rate between the Obj-SCI+ group and HC− group (medial pathway: $p = 0.561$; lateral pathway: $p = 0.215$) or between the Obj-SCI− group and HC− group (medial pathway: $p = 0.320$; lateral pathway: $p = 0.104$), as demonstrated in Fig. 3D–F.

3.4. Association between cholinergic indices and Aβ aggregation and WMH burden

As shown in Table 2, linear regression analyses revealed significant correlations between normalized NBM volume and cerebral Aβ levels ($\beta = -0.216$, $p = 0.048$) and WMH volume ($\beta = -0.280$, $p = 0.009$). Furthermore, MD in both cholinergic pathways showed a significant association with WMH volume (medial pathway: $\beta = 0.471$, $p < 0.001$; lateral pathway: $\beta = 0.511$, $p < 0.001$) while not being related to cerebral Aβ levels (medial pathway: $\beta = 0.009$, $p = 0.933$; lateral pathway: $\beta = -0.062$, $p = 0.566$).

3.5. Association between cholinergic indices and cognitive performance

As shown in Table 3, normalized NBM volume was significantly correlated with MMSE ($r = 0.290$, $p = 0.004$) and TMT-B ($r = -0.224$, $p = 0.027$), while MD in cholinergic pathways was positively associated with TMT-A (medial pathway: $r = 0.218$, $p = 0.031$; lateral pathway: $r = 0.204$, $p = 0.044$) after controlling for age, sex, education, and *APOE* genotype.

4. Discussion

In this study, we investigated the alterations of the cholinergic NBM and WM pathways in individuals with Obj-SCI, both cross-sectionally and longitudinally. Our results showed that Obj-SCI individuals had a decrease in both NBM volume and integrity of the medial pathway, although no significant difference was found in the lateral pathway compared to HC. Similar results were also observed in Obj-SCI+ individuals. Notably, we also observed reduced integrity of the medial pathway in Obj-SCI− individuals relative to HC−. Our longitudinal analysis revealed the deterioration of normalized NBM volume and cholinergic pathways integrity over time. In particular, Obj-SCI+ individuals exhibited a steeper longitudinal decline in normalized NBM volume compared to HC−. Moreover, our results highlighted the correlation between normalized NBM volume and both amyloid aggregation and WMH burden, as well as between cholinergic pathways integrity and WMH burden. Overall, this study provides comprehensive insight into cholinergic system degeneration in the preclinical stage of AD, which may be a crucial target for early therapeutic interventions.

Previous research has reported cholinergic NBM degeneration, including volume reduction, in the preclinical stage of AD (Nemy et al.,

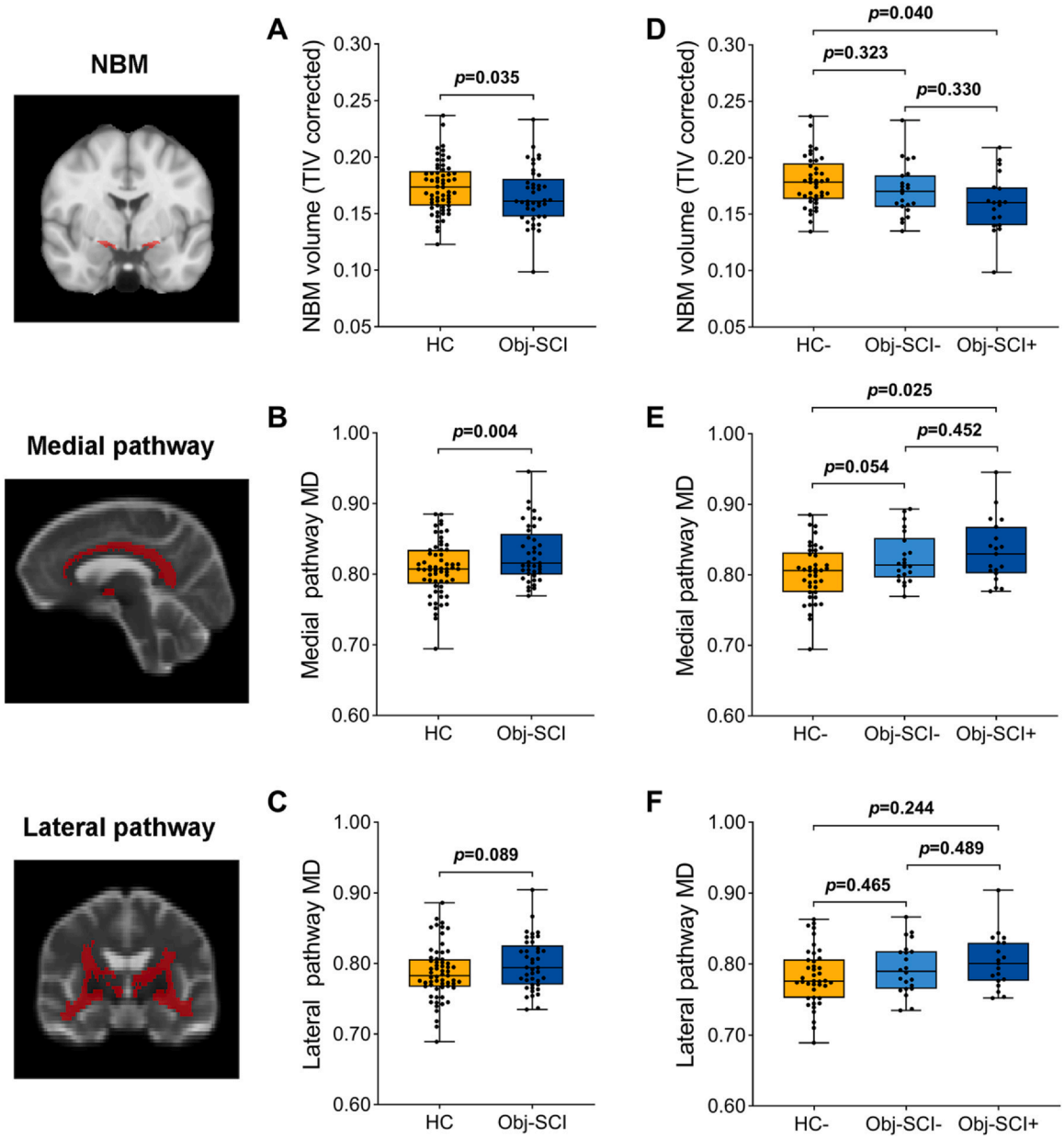

Fig. 2. Group comparison of cholinergic NBM volume and WM pathways integrity at baseline. The masks of NBM, medial pathway, and lateral pathway were shown in the left column, respectively. Cholinergic indices were compared between HC and Obj-SCI groups (A-C), as well as between the amyloid-stratified subgroups (D-F). Abbreviations: HC, healthy controls; MD, mean diffusivity; NBM, nucleus basalis of Meynert; Obj-SCI, objective subtle cognitive impairment; TIV, total intracranial volume.

2023; Scheef et al., 2019). The present study further confirmed the reduction of NBM volume in Obj-SCI individuals compared to HC. Moreover, we found that the decrease in NBM volume evidenced a significant association with lower scores in global cognition and executive function, emphasizing its crucial role in cognitive function (Auld et al., 2002). We also discovered that individuals with Obj-SCI presented impaired integrity of the medial pathway (cingulum), in addition to NBM atrophy, when compared to HC. This result is congruent with a recent study that implemented DTI, which found a reduction in the integrity of the medial pathway among individuals with SCD (Nemy et al., 2023). Nevertheless, we did not observe altered integrity of the lateral pathway (external capsule) in individuals with Obj-SCI compared to HC. Previous DTI studies (Bozzali et al., 2012; Zhang et al., 2007) have consistently shown that selective degeneration occurs along specific fiber pathways during the development of AD, specifically the cingulum. Anatomically, the cingulum connects the medial frontal cortex, medial temporal lobe, and posterior cingulate (Wakana et al., 2004). These regions, which are considered to be the hubs of the default-mode network, are particularly susceptible to AD, which can manifest as functional disconnection (Greicius et al., 2004), atrophy (Dickerson et al., 2009), and higher amyloid deposition (Palmqvist et al., 2017). Additionally, our study found that reduced integrity of cholinergic pathways was positively correlated with a decline in attention function. This corroborates findings from a systematic review, which suggested that attention is the primary cognitive domain mediated by cholinergic pathways (Ballinger et al., 2016). Overall, our study has demonstrated early degeneration of both the NBM and cholinergic medial pathway during the preclinical stage of AD. These findings are particularly significant, as they point to the role that this degeneration plays in early cognitive impairment.

The analysis of amyloid-stratified subgroups showed that Obj-SCI + individuals had reduced NBM volume and integrity of the medial

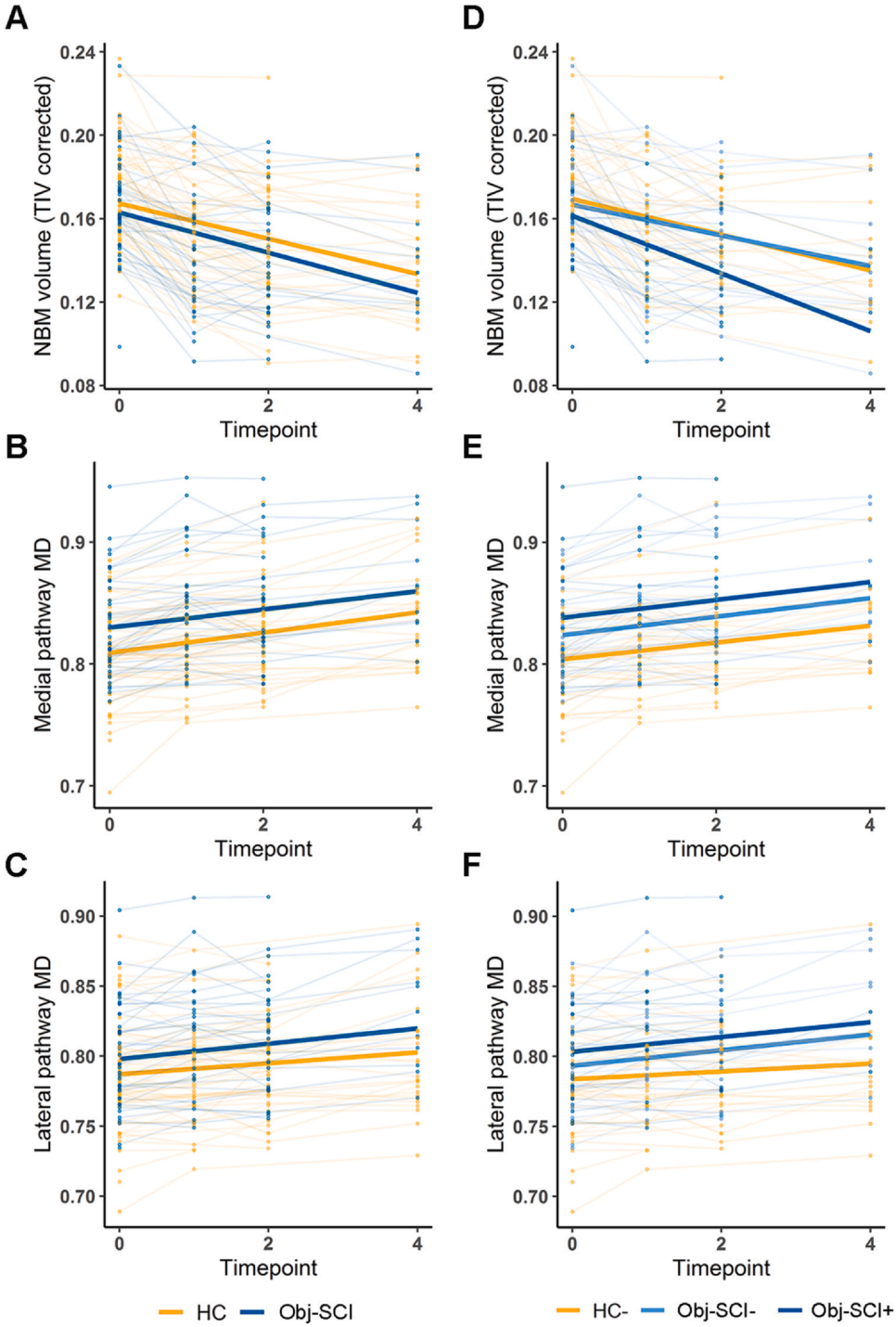

Fig. 3. Longitudinal changes of NBM volume and WM pathways integrity. (A-C) The longitudinal evolutionary trajectories of NBM volume and WM pathways integrity between HC and Obj-SCI groups. (D-F) The longitudinal evolutionary trajectories of cholinergic indices between the amyloid-stratified subgroups. The thin lines represent the changes in individual cholinergic indices over time, and the corresponding thick lines represent the estimated average cholinergic indices changes between groups. The time point on the *X*-axis refers to the year. Abbreviations: HC, healthy controls; MD, mean diffusivity; NBM, nucleus basalis of Meynert; Obj-SCI, objective subtle cognitive impairment; TIV, total intracranial volume.

pathway when compared to HC−. These results further confirm that early cholinergic degeneration is present in the preclinical phase of biologically defined AD. Moreover, this study found that Obj-SCI− individuals also had reduced integrity in the medial pathway compared to HC−. This indicated that the integrity of the medial pathway was compromised before reaching the threshold for pathological accumulation of Aβ. A previous study by Schmitz and Nathan Spreng (2016) involving a large cohort of older adults ranging from cognitively normal to AD found that the degeneration of BF occurred prior to the cortical spread of Alzheimer's pathology, which supports our result. Notably, subthreshold Aβ accumulation has received significant attention due to its predictive value for

Table 2
Linear regression of cholinergic indices associated with Aβ aggregation and WMH burden

	Normalized NBM volume		Medial pathway MD		Lateral pathway MD	
	β	*p*-value	β	*p*-value	β	*p*-value
Age	−0.210	0.058	0.127	0.244	0.063	0.567
Sex	−0.147	0.123	0.117	0.212	0.100	0.290
Education	−0.034	0.722	−0.013	0.888	−0.042	0.656
APOE genotype	−0.018	0.861	−0.119	0.251	−0.103	0.327
Cerebral Aβ levels	**−0.216**	**0.048**	0.009	0.933	−0.062	0.566
WMH volume	**−0.280**	**0.009**	**0.471**	**< 0.001**	**0.511**	**< 0.001**

Standard β-coefficients were shown.
Key: Aβ, amyloid beta; MD, mean diffusivity; NBM, nucleus basalis of Meynert; WMH, white matter hyperintensities.
Values in bold indicate $p < 0.05$.

future cognitive decline and tau deposition (Farrell et al., 2021; Landau et al., 2018; Leal et al., 2018) in cognitively normal adults. A recent study reported that subthreshold level of Aβ deposition was also associated with dementia conversion in Aβ− amnestic MCI patients (Kim et al., 2022). However, we did not observe any significant difference in NBM volume between Obj-SCI− individuals and HC−. Previous studies have indicated that the integrity of the cholinergic pathways plays a more significant role in cognition in normal aging (Nemy et al., 2020) and the MCI-to-dementia conversion (Schumacher et al., 2022), compared to NBM volume. Furthermore, a recent study (Nemy et al., 2023) proposed a posterior-anterior pattern of cholinergic degeneration, suggesting that the cholinergic system deteriorates earlier in the WM pathways than in the NBM, which follows in the more advanced stages of AD.

To the best of our knowledge, this is the first study to systematically examine longitudinal changes in the integrity of the cholinergic system during the preclinical stage of AD. Prior follow-up studies (Grothe et al., 2013; Machado et al., 2020) have demonstrated faster progression of NBM/BF atrophy in patients with MCI and AD compared to HC. Our current study extends these findings by showing a faster longitudinal decline of NBM volume in Obj-SCI + individuals than HC−. However, we did not observe differences in the rate of degeneration of cholinergic WM pathways between Obj-SCI and its subgroups with HC, which could be attributed to the short follow-up period. Future studies with a longer follow-up period are necessary to examine the longitudinal changes of cholinergic WM pathways in the early stage of AD.

Additionally, we observed that NBM atrophy was associated with an increased Aβ burden. Animal model (Boncristiano et al., 2002), histopathologic study (Arendt et al., 1985), and in vivo neuroimaging studies (Grothe et al., 2014; Kerbler et al., 2015) have increasingly highlighted the close correlation between cholinergic NBM dysfunction and Aβ accumulation, which supports our results. Surprisingly, we also found a negative association between lower NBM volume and higher WMH burden. The relationship between NBM volume and WMH has rarely been studied, except for a recent study that reported similar results in cognitively normal individuals (Nemy et al., 2020). Previous studies (Capizzano et al., 2004; Dadar et al., 2022) have consistently reported that WMH burden is significantly associated with cortical atrophy in AD. Hence, besides amyloid pathology, we believe that vascular injury may also contribute to neuronal loss in the NBM.

The integrity of cholinergic WM pathways showed a significant association with WMH burden, rather than Aβ aggregation, indicating that vascular injury plays a crucial role in the degeneration of cholinergic WM pathways. In cognitively normal individuals, a high WMH burden was associated with lower integrity of the cholinergic pathways (Nemy et al., 2020), which supports our result. Furthermore, Cedres et al. (2022) found that WMH burden is a more critical factor than the Aβ42/40 ratio and phosphorylated tau levels in CSF in contributing to the degeneration of cholinergic pathways in cognitively unimpaired individuals. However, in contrast to the aforementioned findings, Nemy et al. (2023) observed a significant correlation between the integrity of the cholinergic WM pathways with CSF levels of Aβ42/40 and tau in the AD continuum. A plausible explanation for this discrepancy is that degeneration of the cholinergic pathway may be caused by WMH lesions in the early stage of AD that worsen in the late stages with the increased accumulation of AD pathological biomarkers. Future studies should further investigate the specific roles of WMH burden and AD pathological biomarkers in cholinergic pathways degeneration in the AD continuum.

5. Limitations

The present study has several limitations. Firstly, based on its design, the participants recruited from the ADNI database were mostly white, highly educated, and healthy individuals. The inherent selection bias in ADNI may prevent our findings from being generalized to the entire population, because race/ethnicity, culture, and education level are important risk factors associated with AD and related dementias. Moreover, the difference in medial pathway MD between the Obj-SCI− group and HC− group was close to statistical

Table 3
Association between cholinergic indices and cognitive performance

	Normalized NBM volume		Medial pathway MD		Lateral pathway MD	
	r	*p*-value	r	*p*-value	r	*p*-value
MMSE	**0.290**	**0.004**	−0.033	0.746	−0.044	0.667
AVLT delayed recall	0.077	0.450	−0.138	0.176	−0.135	0.185
AVLT recognition	−0.004	0.972	−0.023	0.823	−0.060	0.556
TMT-A (s)	0.024	0.814	**0.218**	**0.031**	**0.204**	**0.044**
TMT-B (s)	**−0.224**	**0.027**	0.029	0.773	−0.021	0.840
SVF	0.053	0.606	−0.176	0.082	−0.137	0.177
BNT	0.115	0.258	−0.065	0.528	−0.004	0.967

Key: AVLT, auditory verbal learning test; BNT, Boston naming test; MD, mean diffusivity; MMSE, mini-mental state examination; NBM, nucleus basalis of Meynert; SVF, semantic verbal fluency; TMT, trail-making test.
Values in bold indicate $p < 0.05$.

significance ($p = 0.054$), which may be due to the small sample size. Thus, we appreciate population-based cohorts with a larger sample size to validate our findings. Secondly, despite the longitudinal design of this study, the follow-up period was limited to 48 months, during which time the microstructure of cholinergic WM pathways did not change. Future studies with a longer follow-up period are necessary to explore the longitudinal changes of the cholinergic system in the preclinical stage of AD. Finally, this study lacked molecular data specific to the cholinergic system. There is evidence that cholinergic PET links WM lesions to the cortical cholinergic system in individuals without dementia (Bohnen et al., 2009) and in patients with MCI due to AD (Richter et al., 2017). Studies based on PET imaging are needed to explore the cortical cholinergic change in the early stage of AD.

6. Conclusions

Our study contributes to the existing knowledge by demonstrating the degeneration of NBM and cholinergic medial pathway in individuals with Obj-SCI, which significantly impacts cognitive function. Moreover, we found that the decline in cholinergic medial pathway integrity may start even at subthreshold Aβ levels, followed by NBM atrophy as Aβ levels increase in the preclinical stage of AD. Furthermore, our findings suggest that different pathological processes, such as amyloid accumulation and vascular injury, may have varying contributions to NBM atrophy and reduced integrity of WM pathways in the early stage of AD. Our study highlights novel biomarkers for the preclinical stage of AD and provides insights into early therapeutic interventions.

Ethics approval and consent to participate

All procedures performed in studies involving human participants were in accordance with the ethical standards of the institutional and/or national research committee and with the 1964 Helsinki declaration and its later amendments or comparable ethical standards. Written informed consent was obtained from all participants and/or authorized representatives.

Declaration of generative AI in scientific writing

The authors declare that they do not use AI and AI-assisted technologies in their manuscript.

CRediT authorship contribution statement

TTQ and HH conceptualized the study, analyzed the data, and drafted the manuscript (equal). QZZ collected clinical and imaging data. XL participated in statistical analysis. XHW, PYH, SPD, and MMZ contributed to the conceptualization of the study. XPX, FX, XDL, and KCL contributed to the data interpretation. All authors participated in the revision of the paper and approved the final published version.

Disclosure statement

The authors declare that they have no competing interests.

Acknowledgements

This study was funded by the Linyi Science and Technology Development Program (Grant No. 2022YX0005) and National Natural Science Foundation of China (Grant Nos. 82271936 and 82202090). The data collection and sharing for this project were funded by the Alzheimer's disease neuroimaging initiative (National Institutes of Health Grant U01 AG024904) and Department of Defense Alzheimer's disease neuroimaging initiative (Award No. W81XWH-12–2-0012).

Submission declaration and verification

We certify that all the authors have read the papers and have agreed to be listed as authors. The authors have no conflicts of interest to disclose. The data contained in the manuscript being submitted have not been previously published, have not been submitted elsewhere, and will not be submitted elsewhere while under consideration at Neurobiology of Aging.

Supplementary material

Supplementary data associated with this article can be found in the online version at doi:10.1016/j.neurobiolaging.2023.09.011.

References

Arendt, T., Bigl, V., Tennstedt, A., Arendt, A., 1985. Neuronal loss in different parts of the nucleus basalis is related to neuritic plaque formation in cortical target areas in Alzheimer's disease. Neuroscience 14 (1), 1–14. https://doi.org/10.1016/0306-4522(85)90160-5

Ashburner, J., Friston, K., 2007. Non-linear registration. Statistical Parametric Mapping. Academic Press, New York, NY.

Auld, D.S., Kornecook, T.J., Bastianetto, S., Quirion, R., 2002. Alzheimer's disease and the basal forebrain cholinergic system: relations to beta-amyloid peptides, cognition, and treatment strategies. Prog. Neurobiol. 68 (3), 209–245. https://doi.org/10.1016/s0301-0082(02)00079-5

Avants, B.B., Epstein, C.L., Grossman, M., Gee, J.C., 2008. Symmetric diffeomorphic image registration with cross-correlation: evaluating automated labeling of elderly and neurodegenerative brain. Med. Image Anal. 12 (1), 26–41. https://doi.org/10.1016/j.media.2007.06.004

Ballinger, E.C., Ananth, M., Talmage, D.A., Role, L.W., 2016. Basal forebrain cholinergic circuits and signaling in cognition and cognitive decline. Neuron 91 (6), 1199–1218. https://doi.org/10.1016/j.neuron.2016.09.006

Bates, D., Mchler, M., Bolker, B.M., Walker, S., 2015. Fitting linear mixed-effects models using lme4. Foundation for Open Access Statistics. doi:10.18637/JSS.V067.I01.

Bohnen, N.I., Müller, M.L., Kuwabara, H., Constantine, G.M., Studenski, S.A., 2009. Age-associated leukoaraiosis and cortical cholinergic deafferentation. Neurology 72 (16), 1411–1416. https://doi.org/10.1212/WNL.0b013e3181a187c6

Boncristiano, S., Calhoun, M.E., Kelly, P.H., Pfeifer, M., Bondolfi, L., Stalder, M., Phinney, A.L., Abramowski, D., Sturchler-Pierrat, C., Enz, A., Sommer, B., Staufenbiel, M., Jucker, M., 2002. Cholinergic changes in the APP23 transgenic mouse model of cerebral amyloidosis. J. Neurosci. 22 (8), 3234–3243. https://doi.org/10.1523/jneurosci.22-08-03234.2002

Bondi, M.W., Edmonds, E.C., Jak, A.J., Clark, L.R., Delano-Wood, L., McDonald, C.R., Nation, D.A., Libon, D.J., Au, R., Galasko, D., Salmon, D.P., 2014. Neuropsychological criteria for mild cognitive impairment improves diagnostic precision, biomarker associations, and progression rates. J. Alzheimers Dis. 42 (1), 275–289. https://doi.org/10.3233/jad-140276

Bozzali, M., Giulietti, G., Basile, B., Serra, L., Spano, B., Perri, R., Giubilei, F., Marra, C., Caltagirone, C., Cercignani, M., 2012. Damage to the cingulum contributes to Alzheimer's disease pathophysiology by deafferentation mechanism. Hum. Brain Mapp. 33 (6), 1295–1308. https://doi.org/10.1002/hbm.21287

Brueggen, K., Dyrba, M., Barkhof, F., Hausner, L., Filippi, M., Nestor, P.J., Hauenstein, K., Klöppel, S., Grothe, M.J., Kasper, E., Teipel, S.J., 2015. Basal forebrain and hippocampus as predictors of conversion to Alzheimer's disease in patients with mild cognitive impairment - a multicenter DTI and volumetry study. J. Alzheimers Dis. 48 (1), 197–204. https://doi.org/10.3233/jad-150063

Cantero, J.L., Zaborszky, L., Atienza, M., 2017. Volume loss of the nucleus basalis of Meynert is associated with atrophy of innervated regions in mild cognitive impairment. Cereb. Cortex 27 (8), 3881–3889. https://doi.org/10.1093/cercor/bhw195

Capizzano, A.A., Ación, L., Bekinschtein, T., Furman, M., Gomila, H., Martínez, A., Mizrahi, R., Starkstein, S.E., 2004. White matter hyperintensities are significantly associated with cortical atrophy in Alzheimer's disease. J. Neurol. Neurosurg. Psychiatry 75 (6), 822–827. https://doi.org/10.1136/jnnp.2003.019273

Cedres, N., Ferreira, D., Nemy, M., Machado, A., Pereira, J.B., Shams, S., Wahlund, L.O., Zettergren, A., Stepankova, O., Vyslouzilova, L., Eriksdotter, M., Teipel, S., Grothe, M.J., Blennow, K., Zetterberg, H., Scholl, M., Kern, S., Skoog, I., Westman, E., 2022. Association of cerebrovascular and Alzheimer disease biomarkers with cholinergic white matter degeneration in cognitively unimpaired individuals. Neurology 99 (15), e1619–e1629. https://doi.org/10.1212/WNL.0000000000200930

Dadar, M., Manera, A.L., Ducharme, S., Collins, D.L., 2022. White matter hyperintensities are associated with grey matter atrophy and cognitive decline in Alzheimer's disease and frontotemporal dementia. Neurobiol. Aging 111, 54–63. https://doi.org/10.1016/j.neurobiolaging.2021.11.007

Dhollander, T., Connelly, A., 2016. A novel iterative approach to reap the benefits of multi-tissue CSD from just single-shell (+b=0) diffusion MRI data. Proceedings of the 24th International Society of Magnetic Resonance in Medicine. Singapore, pp. 3010.

Dhollander, T., Raffelt, D., Connelly, A., 2016. Unsupervised 3-tissue response function estimation from single-shell or multi-shell diffusion MR data without a co-registered T1 image. Proceedings of the ISMRM Workshop on Breaking the Barriers of Diffusion MRI. Lisbon, Portugal, pp. 5.

Dickerson, B.C., Bakkour, A., Salat, D.H., Feczko, E., Pacheco, J., Greve, D.N., Grodstein, F., Wright, C.I., Blacker, D., Rosas, H.D., Sperling, R.A., Atri, A., Growdon, J.H., Hyman, B.T., Morris, J.C., Fischl, B., Buckner, R.L., 2009. The cortical signature of Alzheimer's disease: regionally specific cortical thinning relates to symptom severity in very mild to mild AD dementia and is detectable in asymptomatic amyloid-positive individuals. Cereb. Cortex 19 (3), 497–510. https://doi.org/10.1093/cercor/bhn113

Dubois, B., Hampel, H., Feldman, H.H., Scheltens, P., Aisen, P., Andrieu, S., Bakardjian, H., Benali, H., Bertram, L., Blennow, K., Broich, K., Cavedo, E., Crutch, S., Dartigues, J.F., Duyckaerts, C., Epelbaum, S., Frisoni, G.B., Gauthier, S., Genthon, R., Gouw, A.A., Habert, M.O., Holtzman, D.M., Kivipelto, M., Lista, S., Molinuevo, J.L., O'Bryant, S.E., Rabinovici, G.D., Rowe, C., Salloway, S., Schneider, L.S., Sperling, R., Teichmann, M., Carrillo, M.C., Cummings, J., Jack Jr, C.R., 2016. Preclinical Alzheimer's disease: definition, natural history, and diagnostic criteria. Alzheimers Dement. 12 (3), 292–323. https://doi.org/10.1016/j.jalz.2016.02.002

Farrell, M.E., Jiang, S., Schultz, A.P., Properzi, M.J., Price, J.C., Becker, J.A., Jacobs, H.I.L., Hanseeuw, B.J., Rentz, D.M., Villemagne, V.L., Papp, K.V., Mormino, E.C., Betensky, R.A., Johnson, K.A., Sperling, R.A., Buckley, R.F., Alzheimer's Disease Neuroimaging, I, the Harvard Aging Brain, S., 2021. Defining the lowest threshold for amyloid-PET to predict future cognitive decline and amyloid accumulation. Neurology 96 (4), e619–e631. https://doi.org/10.1212/WNL.0000000000011214

Greicius, M.D., Srivastava, G., Reiss, A.L., Menon, V., 2004. Default-mode network activity distinguishes Alzheimer's disease from healthy aging: evidence from functional MRI. Proc. Natl. Acad. Sci. U. S. A. 101 (13), 4637–4642. https://doi.org/10.1073/pnas.0308627101

Grothe, M., Heinsen, H., Teipel, S., 2013. Longitudinal measures of cholinergic forebrain atrophy in the transition from healthy aging to Alzheimer's disease. Neurobiol. Aging 34 (4), 1210–1220. https://doi.org/10.1016/j.neurobiolaging.2012.10.018

Grothe, M., Heinsen, H., Teipel, S.J., 2012. Atrophy of the cholinergic Basal forebrain over the adult age range and in early stages of Alzheimer's disease. Biol. Psychiatry 71 (9), 805–813. https://doi.org/10.1016/j.biopsych.2011.06.019

Grothe, M.J., Ewers, M., Krause, B., Heinsen, H., Teipel, S.J., 2014. Basal forebrain atrophy and cortical amyloid deposition in nondemented elderly subjects. Alzheimers Dement. 10 (5 Suppl), S344–S353. https://doi.org/10.1016/j.jalz.2013.09.011

Hampel, H., Mesulam, M.M., Cuello, A.C., Farlow, M.R., Giacobini, E., Grossberg, G.T., Khachaturian, A.S., Vergallo, A., Cavedo, E., Snyder, P.J., Khachaturian, Z.S., 2018. The cholinergic system in the pathophysiology and treatment of Alzheimer's disease. Brain 141 (7), 1917–1933. https://doi.org/10.1093/brain/awy132

Herdick, M., Dyrba, M., Fritz, H.J., Altenstein, S., Ballarini, T., Brosseron, F., Buerger, K., Can Cetindag, A., Dechent, P., Dobisch, L., Duezel, E., Ertl-Wagner, B., Fliessbach, K., Dawn Freiesleben, S., Frommann, I., Glanz, W., Dylan Haynes, J., Heneka, M.T., Janowitz, D., Kilimann, I., Laske, C., Metzger, C.D., Munk, M.H., Peters, O., Priller, J., Roy, N., Scheffler, K., Schneider, A., Spottke, A., Jakob Spruth, E., Tscheuschler, M., Vukovich, R., Wiltfang, J., Jessen, F., Teipel, S., Grothe, M.J., 2020. Multimodal MRI analysis of basal forebrain structure and function across the Alzheimer's disease spectrum. Neuroimage Clin. 28, 102495. https://doi.org/10.1016/j.nicl.2020.102495

Jak, A.J., Bondi, M.W., Delano-Wood, L., Wierenga, C., Corey-Bloom, J., Salmon, D.P., Delis, D.C., 2009. Quantification of five neuropsychological approaches to defining mild cognitive impairment. Am. J. Geriatr. Psychiatry 17 (5), 368–375. https://doi.org/10.1097/JGP.0b013e31819431d5

Kerbler, G.M., Fripp, J., Rowe, C.C., Villemagne, V.L., Salvado, O., Rose, S., Coulson, E.J., Alzheimer's Disease Neuroimaging, I., 2015. Basal forebrain atrophy correlates with amyloid beta burden in Alzheimer's disease. Neuroimage Clin. 7, 105–113. https://doi.org/10.1016/j.nicl.2014.11.015

Kilimann, I., Grothe, M., Heinsen, H., Alho, E.J., Grinberg, L., Amaro Jr., E., Dos Santos, G.A., da Silva, R.E., Mitchell, A.J., Frisoni, G.B., Bokde, A.L., Fellgiebel, A., Filippi, M., Hampel, H., Klöppel, S., Teipel, S.J., 2014. Subregional basal forebrain atrophy in Alzheimer's disease: a multicenter study. J. Alzheimers Dis. 40 (3), 687–700. https://doi.org/10.3233/jad-132345

Kim, H.J., Oh, J.S., Lim, J.S., Lee, S., Jo, S., Chung, E.N., Shim, W.H., Oh, M., Kim, J.S., Roh, J.H., Lee, J.H., Alzheimer's Disease Neuroimaging, I., 2022. The impact of subthreshold levels of amyloid deposition on conversion to dementia in patients with amyloid-negative amnestic mild cognitive impairment. Alzheimers Res. Ther. 14 (1), 93. https://doi.org/10.1186/s13195-022-01035-2

Landau, S.M., Horng, A., Jagust, W.J., Alzheimer's Disease Neuroimaging, I., 2018. Memory decline accompanies subthreshold amyloid accumulation. Neurology 90 (17), e1452–e1460. https://doi.org/10.1212/WNL.0000000000005354

Landau, S.M., Mintun, M.A., Joshi, A.D., Koeppe, R.A., Petersen, R.C., Aisen, P.S., Weiner, M.W., Jagust, W.J., Alzheimer's Disease Neuroimaging, I., 2012. Amyloid deposition, hypometabolism, and longitudinal cognitive decline. Ann. Neurol. 72 (4), 578–586. https://doi.org/10.1002/ana.23650

Leal, S.L., Lockhart, S.N., Maass, A., Bell, R.K., Jagust, W.J., 2018. Subthreshold amyloid predicts tau deposition in aging. J. Neurosci. 38 (19), 4482–4489. https://doi.org/10.1523/JNEUROSCI.0485-18.2018

Liu, A.K., Chang, R.C., Pearce, R.K., Gentleman, S.M., 2015. Nucleus basalis of Meynert revisited: anatomy, history and differential involvement in Alzheimer's and Parkinson's disease. Acta Neuropathol. 129 (4), 527–540. https://doi.org/10.1007/s00401-015-1392-5

Machado, A., Ferreira, D., Grothe, M.J., Eyjolfsdottir, H., Almqvist, P.M., Cavallin, L., Lind, G., Linderoth, B., Seiger, A., Teipel, S., Wahlberg, L.U., Wahlund, L.O., Westman, E., Eriksdotter, M., Alzheimer's Disease Neuroimaging, I., 2020. The cholinergic system in subtypes of Alzheimer's disease: an in vivo longitudinal MRI study. Alzheimers Res. Ther. 12 (1), 51. https://doi.org/10.1186/s13195-020-00620-7

Nemy, M., Cedres, N., Grothe, M.J., Muehlboeck, J.S., Lindberg, O., Nedelska, Z., Stepankova, O., Vyslouzilova, L., Eriksdotter, M., Barroso, J., Teipel, S., Westman, E., Ferreira, D., 2020. Cholinergic white matter pathways make a stronger contribution to attention and memory in normal aging than cerebrovascular health and nucleus basalis of Meynert. Neuroimage 211, 116607. https://doi.org/10.1016/j.neuroimage.2020.116607

Nemy, M., Dyrba, M., Brosseron, F., Buerger, K., Dechent, P., Dobisch, L., Ewers, M., Fliessbach, K., Glanz, W., Goerss, D., Heneka, M.T., Hetzer, S., Incesoy, E.I., Janowitz, D., Kilimann, I., Laske, C., Maier, F., Munk, M.H., Perneczky, R., Peters, O., Preis, L., Priller, J., Rauchmann, B.S., Röske, S., Roy, N., Scheffler, K., Schneider, A., Schott, B.H., Spottke, A., Spruth, E.J., Wagner, M., Wiltfang, J., Yakupov, R., Eriksdotter, M., Westman, E., Stepankova, O., Vyslouzilova, L., Düzel, E., Jessen, F., Teipel, S.J., Ferreira, D., 2023. Cholinergic white matter pathways along the Alzheimer's disease continuum. Brain 146 (5), 2075–2088. https://doi.org/10.1093/brain/awac385

Palmqvist, S., Schöll, M., Strandberg, O., Mattsson, N., Stomrud, E., Zetterberg, H., Blennow, K., Landau, S., Jagust, W., Hansson, O., 2017. Earliest accumulation of β-amyloid occurs within the default-mode network and concurrently affects brain connectivity. Nat. Commun. 8 (1), 1214. https://doi.org/10.1038/s41467-017-01150-x

Qiu, T., Zeng, Q., Zhang, Y., Luo, X., Xu, X., Li, X., Shen, Z., Li, K., Wang, C., Huang, P., Zhang, M., Dai, S., Xie, F., Alzheimer's Disease Neuroimaging, I., 2022. Altered functional connectivity pattern of hippocampal subfields in individuals with objectively-defined subtle cognitive decline and its association with cognition and cerebrospinal fluid biomarkers. Eur. J. Neurosci. 56 (12), 6227–6238. https://doi.org/10.1111/ejn.15860

Richter, N., Michel, A., Onur, O.A., Kracht, L., Dietlein, M., Tittgemeyer, M., Neumaier, B., Fink, G.R., Kukolja, J., 2017. White matter lesions and the cholinergic deficit in aging and mild cognitive impairment. Neurobiol. Aging 53, 27–35. https://doi.org/10.1016/j.neurobiolaging.2017.01.012

Scheef, L., Grothe, M.J., Koppara, A., Daamen, M., Boecker, H., Biersack, H., Schild, H.H., Wagner, M., Teipel, S., Jessen, F., 2019. Subregional volume reduction of the cholinergic forebrain in subjective cognitive decline (SCD). Neuroimage Clin. 21, 101612. https://doi.org/10.1016/j.nicl.2018.101612

Schmidt, P., Gaser, C., Arsic, M., Buck, D., Förschler, A., Berthele, A., Hoshi, M., Ilg, R., Schmid, V.J., Zimmer, C., Hemmer, B., Mühlau, M., 2012. An automated tool for detection of FLAIR-hyperintense white-matter lesions in multiple sclerosis. Neuroimage 59 (4), 3774–3783. https://doi.org/10.1016/j.neuroimage.2011.11.032

Schmitz, T.W., Nathan Spreng, R., 2016. Basal forebrain degeneration precedes and predicts the cortical spread of Alzheimer's pathology. Nat. Commun. 7, 13249. https://doi.org/10.1038/ncomms13249

Schumacher, J., Ray, N.J., Hamilton, C.A., Bergamino, M., Donaghy, P.C., Firbank, M., Watson, R., Roberts, G., Allan, L., Barnett, N., O'Brien, J.T., Thomas, A.J., Taylor, J.P., 2023. Free water imaging of the cholinergic system in dementia with Lewy bodies and Alzheimer's disease. Alzheimers Dement. 19 (10), 4549–4563. https://doi.org/10.1002/alz.13034

Schumacher, J., Ray, N.J., Hamilton, C.A., Donaghy, P.C., Firbank, M., Roberts, G., Allan, L., Durcan, R., Barnett, N., O'Brien, J.T., Taylor, J.P., Thomas, A.J., 2022. Cholinergic white matter pathways in dementia with Lewy bodies and Alzheimer's disease. Brain 145 (5), 1773–1784. https://doi.org/10.1093/brain/awab372

Selden, N.R., Gitelman, D.R., Salamon-Murayama, N., Parrish, T.B., Mesulam, M.M., 1998. Trajectories of cholinergic pathways within the cerebral hemispheres of the human brain. Brain 121 (Pt 12), 2249–2257. https://doi.org/10.1093/brain/121.12.2249

Teipel, S.J., Cavedo, E., Hampel, H., Grothe, M.J., 2018. Basal forebrain volume, but not hippocampal volume, is a predictor of global cognitive decline in patients with Alzheimer's disease treated with cholinesterase inhibitors. Front. Neurol. 9, 642. https://doi.org/10.3389/fneur.2018.00642

Thomas, K.R., Bangen, K.J., Weigand, A.J., Edmonds, E.C., Wong, C.G., Cooper, S., Delano-Wood, L., Bondi, M.W., 2020. Objective subtle cognitive difficulties predict future amyloid accumulation and neurodegeneration. Neurology 94 (4), e397–e406. https://doi.org/10.1212/wnl.0000000000008838

Thomas, K.R., Edmonds, E.C., Eppig, J., Salmon, D.P., Bondi, M.W., 2018. Using neuropsychological process scores to identify subtle cognitive decline and predict progression to mild cognitive impairment. J. Alzheimers Dis. 64 (1), 195–204. https://doi.org/10.3233/jad-180229

Wakana, S., Jiang, H., Nagae-Poetscher, L.M., van Zijl, P.C., Mori, S., 2004. Fiber tract-based atlas of human white matter anatomy. Radiology 230 (1), 77–87. https://doi.org/10.1148/radiol.2301021640

Whitehouse, P.J., Price, D.L., Clark, A.W., Coyle, J.T., DeLong, M.R., 1981. Alzheimer disease: evidence for selective loss of cholinergic neurons in the nucleus basalis. Ann. Neurol. 10 (2), 122–126. https://doi.org/10.1002/ana.410100203

Whitehouse, P.J., Price, D.L., Struble, R.G., Clark, A.W., Coyle, J.T., Delon, M.R., 1982. Alzheimer's disease and senile dementia: loss of neurons in the basal forebrain. Science 215 (4537), 1237–1239. https://doi.org/10.1126/science.7058341

Zhang, Y., Schuff, N., Jahng, G.H., Bayne, W., Mori, S., Schad, L., Mueller, S., Du, A.T., Kramer, J.H., Yaffe, K., Chui, H., Jagust, W.J., Miller, B.L., Weiner, M.W., 2007. Diffusion tensor imaging of cingulum fibers in mild cognitive impairment and Alzheimer disease. Neurology 68 (1), 13–19. https://doi.org/10.1212/01.wnl.0000250326.77323.01